Journal of Applied Research in Water and Wastewater
E-ISSN: 2476-6283
Journal homepage: https://arww.razi.ac.ir

# Mixing characteristic improvement of a wastewater treatment plant anerobic digester using CFD analysis

**Seyed Hosein Arabfarashahi, Shahram Talebi***

*Department of Mechanical Engineering, Faculty of Mechanical Engineering, Yazd University, Yazd, Iran.*

## GRAPHICAL ABSTRACT

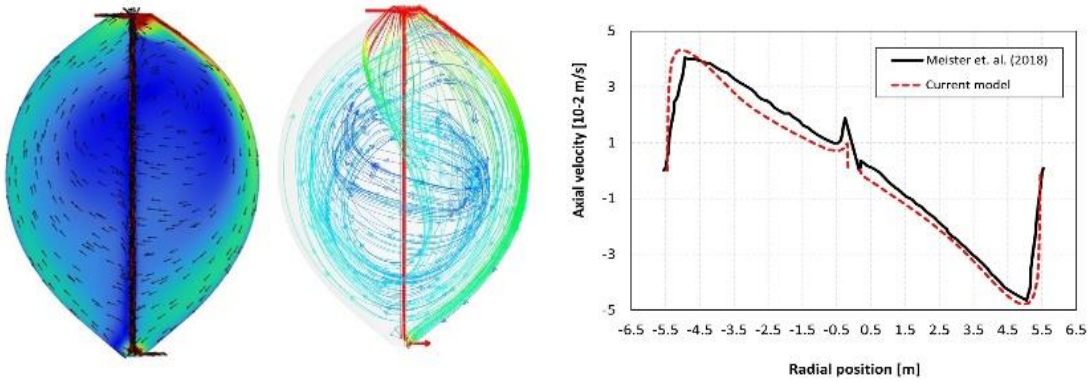


## ARTICLE INFO

**Article type:**
Research Article

**Article history:**
Received 21 May 2025
Received in revised form 2 August 2025
Accepted 8 August 2025
Available online 30 December 2025

**Keywords:**
Computational fluid dynamics
Wastewater treatment
Digester modelling



## ABSTRACT

In this paper the influence of the operational and geometrical parameters on the mixing and flow uniformity within an anaerobic digester is investigated. Anaerobic digestion is classified as single or multiphase flow reactor to produce biogas from processed organic waste. Within the digesters, mass transfer is a key component to obtain an optimal process which is highly dependent on uniformity and turbulence of the flow. Two quantitative mixing criteria namely uniformity index and turbulence intensity are assessed to investigate the possibility of improving mixing characteristics of an operating digester. The effect of inlet velocity, draft tube flow presence, draft tube velocity magnitude and direction and inlet tube position have been investigated and compared to a validated base case. According to the finding both inlet velocity and inlet pipe position can noticeably affect the operation of the digester and proper tuning of the inlet velocity and also optimized pipe position can enhance the uniformity of the flow while inducing high turbulence within the digester. Furthermore, by adjusting the inlet pipe position, it is possible to improve the uniformity index and turbulence intensity by 44% and 40% respectively.

## 1. Introduction

Anaerobic digestion (AD) is one of the main and commonly used technologies to produce biogas which is a reliable renewable source of energy (Meister *et al.*, 2018; Wu and Chen, 2008; Wu, 2010). During the process, the organic matter and volatile solids in the medium are broken down into simpler components through intricate biological-chemical-physical processes and in the absence of oxygen (Dabiri *et al.*, 2021; Singh *et al.*, 2021). The high efficiency of the process has made it a viable alternative of treating a wide range of biodegradable sources (Leonzio, 2018; Craig *et al.*, 2013). Proven to be highly efficient and easy to operate, the AD process has been utilized in wastewater treatment plants (WWTP) and sewage treatment and shows a huge potential for large-scale and industrial applications (Zhang *et al.*, 2018; López-Jiménez *et al.*, 2015).

WWTP consists of three main stages. Initially, the liquid material is treated to remove visible and suspended solids. In the second stage, the dissolved organic matter is separated via biological processes. In the third stage the aim is to achieve the highest level of purification by employing advanced technologies to remove additional contaminants or specific pollutants. This is where the AD process is used to reduce the organic leftovers from previous stages. In fact, the AD process stabilizes the sludge and generates biogas as a byproduct making it a valuable tool for sludge treatment and resource recovery. The stabilized sludge can then be utilized or safely disposed of after digestion (López-Jiménez *et al.*, 2015). There have been numerous industrial and laboratory-scale studies of the AD process with different designs and configurations. In general, the main AD tank can be classified into two configurations, namely plug flow (PF) and continuous stirred-tank (CST) digester. The latter is also known as mixed-flow digester (Karim *et al.*, 2004). Compared to plug-flow digesters, mixed-flow digesters offer several advantages, including the efficient use of the entire geometrical volume, lower temperature gradients throughout the volume, and a higher dispersion and better mixing of the byproducts. Combination of these parameters ensures a close interaction between bacteria and the substrate (Wu and Chen, 2008).

*Corresponding author Email: talebi_s@yazd.ac.ir

Cite this article: S.H. Arabfarashahi, S. Talebi, Mixing characteristic improvement of a wastewater treatment plant anerobic digester using CFD analysis, *Journal of Applied Research in Water and Wastewater*, 12 (2), 2025, 210-218. doi: https://doi.org/10.22126/arww.2025.12055.1368

Digesters can be manufactured into different shapes such as rectangular, cylindrical, or egg-shaped. Depending on the level optimization, egg-shaped digesters (ESD) proven to be more efficient, cost-effective digestion systems for sludge treatment. In fact, the ESDs have demonstrated enhanced mixing, and lower generation of dead zones.

This in turn reduces the regular maintenance which usually disturbs the continuous processes for a considerable time (Wu, 2010). Moreover, the ESDs offer a high surface/volume ratio which ultimately reduces construction costs and also the heat losses during the process (Wu, 2010).

There are numerous geometrical and operational factors that affect the performance of an anaerobic digester among which feeding patterns, flow rheology, temperature, retention time, and mixing efficiency are worth mentioning. Of these factors, effective mixing is crucial for optimal operation of a digester (Leonzio, 2018). Good mixing ensures physical, chemical, and biological homogenization, enhancing solid digestion by regulating mass and heat transfer rates, as well as facilitating reactions and structural changes. It prevents solids from settling at the bottom and biomass from floating to the surface (Leonzio, 2018). Therefore, insufficient mixing significantly reduces digestion efficiency (Meroney and Colorado, 2009; Wu, 2014). However, there have been some studies suggesting the mixing efficiency declined at higher mixing intensities which consequently disturbs the spatial distribution of the microorganisms. This is mainly due to a higher shear rate (Singh *et al*., 2021; López-Jiménez *et al*., 2015; Wu and Chen, 2008; Wang *et al*., 2017).

Nevertheless, most of the studies have suggested to minimize the non-uniformity to reduce dead spaces in the digester which ultimately leads to an improvement in the mixing process (Leonzio, 2018; Wu, 2014). From the above-mentioned discussions and literature, the importance of the optimized mixing level becomes evident. Mixing in a mixed-flow digester can be performed via different modes such as slurry recirculation (pumped recirculation), mechanical mixing (impeller and draft tube mixing), and gas recirculation among which mechanical mixing is proven to be the best and most common way for achieving maximum homogenization and mixing efficiency (Wu, 2010; Dabiri *et al*., 2021; Singh *et al*., 2021).

Both experimental and computational methods could be employed to investigate the mixing performance in anaerobic digesters. However, conventional experimental techniques face challenges in measuring flow fields due to the opacity of the processed liquid. To address this, advanced non-invasive methods, such as particle tracking and tracer addition to the liquid have been employed to measure and visualize flow patterns in lab-scale digesters (Wu, 2010).

Even though experimental procedures are usually more reliable and effective, they are often time-consuming, particularly for processes like determining hydraulic retention time. This process usually involves tracking an added tracer at the inlet of the digester and measuring the concentration at the outlet over extended periods. Moreover, experimental methods are limited to available digesters. In contrast, mathematical modeling offers a more efficient alternative, enabling the design and analysis of future digester systems (López-Jiménez *et al*., 2015). As an alternative to the experimental approach, computational fluid dynamics (CFD) has become a well-established and widespread numerical tool for flow analysis. In a CFD model, a set of scalar equations describing mass, energy, momentum, and species exchange phenomena are solved for a specific geometry and boundary conditions. The numerical results are used to visualize and study the flow, temperature, and species concentration patterns to understand different physical and chemical phenomena (Wang *et al*., 2017). Once validated, a CFD model offers a significant advantage over experimental methods by providing details that might be difficult or infeasible through direct measurements, especially for different designs in a much shorter time and lower costs (Wu, 2010; Dabiri *et al*., 2021; Craig *et al*., 2013; Wols *et al*., 2010; Caillet *et al*., 2023). Numerous studies have been successfully carried out using CFD simulation to design and investigated different parameters to improve the AD process performance.

López-Jiménez *et al.* (2015) used a 3D CFD model to analyze the velocity field a flow pattern and to identify possible dead zones within a large-scale wastewater treatment plant anaerobic digester. They employed a single-phase model by considering both Newtonian and non-Newtonian flow behavior. The model is validated by available operational data and their findings highlights the importance of the mixing process in the digester. Ultimately they have proposed different possibilities to reduce the volume of the dead zones to improve the mixing efficiency. In another study, Wu (2010) developed a CFD model validated against power and flow numbers. They utilized the model to compare egg-shaped and cylindrical digesters and reported a better performance for the egg shaped configuration in terms of the mixing efficiency. Furthermore, they reported a more uniform flow using a mechanical draft tube. Using the same validated model, they further optimized the propeller position and rotational direction and ultimately proposed scale-up rules for egg-shaped digesters.

Vesvikar *et al*. (2005) set up and validated a CFD model to utilize gas spargers in an anaerobic digester and to study the flow patterns. Different gas flow rates were tested to see the effects on the circulation pattern, stagnant regions, liquid velocity profiles, and dead zones. They ultimately improved the mixing efficiency and the flow dynamics of the digester by optimizing the draft tube size and tank bottom shapes.

Meroney *et al.* (2009) used a CFD model to study the effect of digester diameter equipped with draft tube mixers on the mixing characteristics. Comparing different calculated parameters, such as digester volume turnover time, hydraulic retention time, and mixture diffusion time, revealed no significant difference in flow pattern and mixing efficiency in different configurations.

Terashima *et al*. (2009) conducted a comprehensive experimental and numerical study on the effect of sludge rheology on mixing efficiency in an anaerobic digester. Using the obtained data from the experiments, they developed mathematical expressions to predict the sludge viscosity. Then the expressions were incorporated in a CFD model to calculate the uniformity index to evaluate the mixing dynamics. They reported a strong dependence of the mixing time on the sludge rheological properties, digester shape, and mixing configurations. Furthermore, the potential of intermittent feeding strategies to improve process efficiency by optimizing feeding cycles based on homogenization time is proposed.

Zhang *et al.* (2018) developed a CFD model to optimize the geometry of a novel high-efficiency anaerobic digester. The digester is a cylindrical-shaped plug flow reactor which has been modified by employing different baffle arrangements to reduce the dead zones and enhance the mixing efficiency along the travel path of the liquid. They reported an improvement in the mixing efficiency by creating a spiral flow inside the digester.

Craig *et al.* (2013) developed a CFD model to evaluate the mechanical mixing in a full-scale anaerobic digester in which mechanical mixing is provided through an impeller located in a draft tube. Utilizing the developed CFD model, they investigated the influence of sewage sludge rheology on the steady-state digester performance.

According to a recent review paper by Caillet *et al*. (2023), most of the available CFD studies have been employed to evaluate the mixing mode or design (75 %), the multiphase study (36 %), the effect of rheology and total solid (TS) content (27 %), and turbulence modeling (18 %).

Moreover, CFD results can be utilized to examine alternative geometries, modifications in the initial geometries, inlet and outlet tube positioning, mixing and pumping configurations (Meroney and Colorado, 2009; Vesvikar and Al-Dahhan, 2005), which can sometimes significantly improve AD process performance (Stamou, 2008).

For instance, Hernández-Aguilar *et al*. (2016) used CFD models to evaluate different recirculation configurations. Sajjadi *et al*. (2016) used a modeled digester reactor to see the possibility of the fluid injectors as a mixing tool. They reported a well-mixed recirculate flow within the tank and emphasized the importance of the inlet and outlet injector location.

López-Jiménez *et al*. (2015) simulated the sludge recycling process as a mixing strategy in a digester tank. They compared different pump inlet shapes, positions, and entrance angles and reported optimization strategies for this kind of configuration.

In this study, a CFD model is developed to study a large-scale egg-shaped digester of a real-life wastewater treatment plant (WWTP). The model is a reproduction of the developed model by Meister *et al.* (2018), which is utilized to investigate the effect of inlet pipe positions, inlet velocity, draft tube velocity, and diameter. Uniformity index and turbulence intensity are the main indicators for performance comparison. As will be discussed in detail, it was found that the position and orientation of the inlet pipes have a considerable effect on the flow pattern and mixing characteristics.

## 2. Theory and model setup

### 2.1. Governing equations

In this section general governing equations are discussed. For more details on the definitions and equations constants the readers are encouraged to are refer to the Ansys Fluent Theory Guide (Ansys, 2013). The equation for conservation of mass in steady state mode, can be written as follows:

$$\nabla \cdot \boldsymbol{v} = 0 \tag{1}$$

where, $v$ is the absolute velocity field within the domain. Coupled with the above equation, momentum is described by

$$\boldsymbol{\rho(v \cdot \nabla)v = -\nabla p + \nabla \cdot \tau + \rho g + S_m} \quad (2)$$

where, $\rho$ is the liquid density (kg/m$^3$), $p$ is pressure (Pa), τ is stress tensor which accounts for shear stress and g is gravitational acceleration vector [m/s$^2$]. $\boldsymbol{S_m}$ is a source term added to the momentum equations to simulate the effects of external forces acting on a fluid, such as those from fans, propellers, or porous media, without explicitly modeling their geometry. It's a way to represent these forces as a volumetric source of momentum within a defined region. In the current study it will be used to define a momentum source to replicate the effect of circulating pump within the digester.

The realizable *k–ϵ* Model is used to include turbulence effect by solving conservation equation for $k$ and $\epsilon$ variables. In the formulations, $k$ is turbulent kinetic energy which is obtained as:

$$\boldsymbol{(v.\nabla)k = \nabla.\left[\left(\eta + \frac{\eta_t}{\sigma_k}\right)\nabla k\right] + P_k - \epsilon} \quad (3)$$

where, k is turbulent kinetic energy [m$^2$/s$^2$], $v$ is velocity vector [m/s], $\eta$ is effective viscosity [m$^2$/s], $\eta_t$ is turbulent viscosity [m$^2$/s], $\sigma_k$ is turbulent Prandtl number, $P_k$ is production of turbulent kinetic energy [m$^2$/s$^3$] and $\epsilon$ is dissipation rate of kinetic energy [m$^2$/s$^3$]. For $\epsilon$ the conservation equation will be:

$$\boldsymbol{(v.\nabla)\epsilon = \nabla.\left[\left(\eta + \frac{\eta_t}{\sigma_\epsilon}\right)\nabla \epsilon\right] + C_1\frac{\epsilon}{k}P_k - C_2\frac{\epsilon^2}{k\sqrt{\eta\epsilon}}} \quad (4)$$

where, $\sigma_\epsilon$ is turbulent Prandtl number for $\epsilon$ and C1 and C2 are empirical constants.

In the above equations $\eta_t$ is turbulent viscosity ($\rho C_\eta \frac{k^2}{\epsilon}$) where $C_\eta$ is the empirical constant. Based on the measurement the applied fluid in the digester acts as a non-Newtonian fluid. In a Newtonian fluid the shear stress is linearly proportional to the shear rate with a proportionality constant that is called molecular viscosity ($\boldsymbol{\eta}$) as written below:

$$\tau = \eta(\nabla v + (\nabla v)^T) \quad (4)$$

However, in a non-Newtonian case, no linear relation can be considered between shear stress and shear rate (Van Canneyt and Verdonck, 2014). Therefore, the viscosity is not a fixed scalar but a variable. In this study, the non-Newtonian viscosity will be modeled based on the power law model which is a well-established relation in hydraulic analysis. This model defines the shear stress as following equation:

$$\boldsymbol{\tau = K(\Upsilon)^n} \quad (5)$$

where, $\tau$ is the shear stress, $\Upsilon$ is the shear rate (or velocity gradient), $K$ is the consistency index and $n$ is the Power Law constants which is a measure of the deviation of the fluid from Newtonian. The Power Law model defines the non-Newtonain viscosity $\eta$ as:

$$\boldsymbol{\eta = K(\Upsilon)^{n-1}} \quad (6)$$

In the Power Law model, a value of $n$ = 1 corresponds to a Newtonian fluid, while 0 < $n$ < 1 is a Shear Thinning (pseudoplastic) fluid and $n$ > 1 represents a Shear Thickening (dilatant) fluid.

### 2.2. Digester configuration and boundary conditions

Fig. **1** shows a 3D schematic view of the digester and the inlet pipe positioning (generated via Ansys SpaceClaim). Detailed dimension of the studied digester can be found in (Meister *et al*., 2018). The digester is equipped with a draft tube inside which a mechanical mixer is installed. The mixer can create downward/upward recirculation in the digester with an average velocity of 1.5 m/s. In the models, the impellers are not included and momentum source are used to reach the defined circulation velocity inside the draft tube.

For the base case with total solid content (TS) of 2.5%, a constant inlet velocity of 1.15 m/s is considered which is calculated based on the corresponding density, inlet area and a constant mass flowrate of 34.6 kg/s. At the inlet boundary condition a hydraulic diameter of 0.2 m and a turbulent intensity of 5% is considered. the TS content within the digester is assumed to be homogenous and equal to the TS at the inlet. A pressure outlet boundary conditions with zero gauge pressure is considered for the outlet boundary condition.

The material properties for the non-Newtonian fluid as a function of total sloid content are reported in Table 1. To mimic the effect of impeller in the draft tube, a momentum source of 85 N/m$^3$ is considered. This value is capable of generating a velocity profile equivalent to the one generated by a 600 rpm impeller which is specified rpm in the study of Meister *et al*. (Meister *et al*., 2018) for TS = 2.5%.

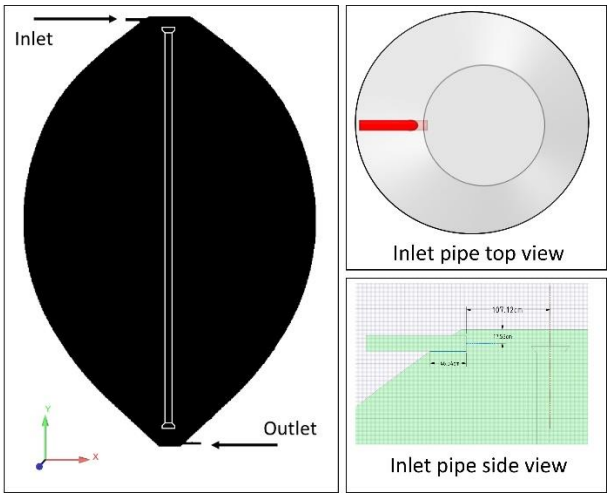


**Fig. 1**. Modelled digester geometry and inlet pipe.

### 2.3. Post processing

Various indices and parameters have been suggested by many researchers to quantify the mixing performance in a mixing equipment (Caillet *et al*., 2023). In this study, the uniformity index (UI) is utilized to predict the mixing dynamics and is defined as follow:

$$\mathbf{UI} = \frac{\sum_{i=1}^{n}(|\boldsymbol{v_i} - \bar{\boldsymbol{v}}|).\boldsymbol{V_i}}{\sum_{i=1}^{n}(\boldsymbol{v_i}.\boldsymbol{V_i})} \quad (7)$$

where, n is number of mesh cell, $v_i$ is cell velocity, $\bar{v}$ is the average velocity in the whole domain and $V_i$ is cell volume.

**Table 1.** Slurry flow physical properties for various *TS* concentrations (Meister *et al*., 2018).

| TS , % | $\rho$ , kg/m$^3$ | K, Pa s$^n$ | n |
|---|---|---|---|
| 0 | 998 | Newtonian | 1 |
| 2.5 | 1000.36 | 4.20E-02 | 0.71 |
| 5.4 | 1000.78 | 1.92E-01 | 0.562 |
| 7.5 | 1001 | 5.25E-01 | 0.533 |
| 9.1 | 1001.31 | 1.05E+00 | 0.467 |
| 12.1 | 1001.73 | 5.89E+00 | 0.367 |

Fig. 2 shows the possible UI values for an average velocity of 0.028 m/s. As can be seen, a computational cell with a value equal to the average velocity will have a UI = 0. As velocity increases; the UI tends to go toward unity. However, for lower cell velocities than average velocity the UI value increases with no limits (greater than one). Therefore, a contour with a UI value greater than 1 indicates a velocity lower than the average velocity.

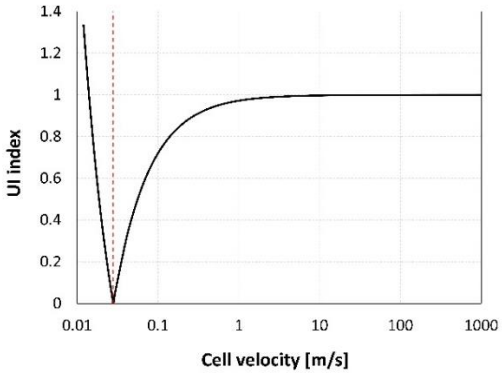


**Fig. 2**. UI values for different cell velocity.

Another parameter which is used in this paper is the turbulent intensity (TI) which is an indicator of the level of intensity inside the digester to achieve proper mixing. In the current study, UI, TI and dead zone parameters are considered for the comparisons.

### 2.4. Solution method

Ansys Fluent software is used to solve the governing equations. SIMPLE scheme is used to couple pressure and velocity in the defined domain. Spatial discretization of gradients is obtained via least

squares cell based approach. All scalar variables are discretized with the second order upwind scheme. The residuals are monitored to attained the residual values of $10^{-4}$.

### 2.5. Case studies

Error! Reference source not found.Table 2 reports the studied cases with descriptive geometries. As can be seen, the effect of inlet velocity, draft tube velocity, pipe numbers, and positions was investigated for a constant mass flow rate. Case A is indeed the base case to which the other cases will be compared. It has the same original geometry of the large-scale digester which is currently in operation. In cases B and C, the effect of inlet velocity is studied, and for cases D and E, the effect of draft tube operation with and without inlet and outlet flow is investigated. Ultimately, in cases F, G, and H, the effect of inlet pipe position on the UI and TI values is reported.

## 3. Results and discussion

### 3.1. Grid independence and model validation

Fig. 3 shows the axial velocity profile (upward velocity) for the base case with and without inlet pump circulation at the horizontal line 6 m above the bottom of the digester. The current CFD model demonstrates strong overall agreement with the literature data reported by Meister *et al.* (2018), capturing the general trend and magnitude of axial velocity across the radial domain. Minor discrepancies, particularly near the central region and domain boundaries, can be attributed to several factors. First, the circulation pump is modeled using a simplified momentum source, which may not fully capture the detailed flow structures generated by a real rotating impeller. Additionally, turbulence modeling, while effective for capturing bulk behavior, relies on closure assumptions that can limit accuracy in regions with strong shear or recirculation. Idealized boundary conditions and geometric assumptions may also contribute to the observed deviations. Finally, it is important to consider that experimental data inherently include measurement uncertainties, which can further account for slight mismatches between the two datasets. Overall, the level of agreement remains within acceptable limits for engineering applications. Fig. 4 shows the result of grid independency studies for 3 different meshes. As can be see there is a minor difference between the profiles, however the finer grids ae closer to each other. The minor differences can also be noticed in the reported values in Table 3. Based on this observations, medium grid (1.5 M) is used for the rest of the analysis.

**Table 2.** Case studies for the digester mixing improvement.

| case | Inlet pipe number | Inlet pipe position | Inlet pipe diameter | Inlet pipe Flow, m/s | Draft tube velocity | Outlet pipe position | Studied variables |
|---|---|---|---|---|---|---|---|
| A (Base Case) | 1 | Middle- Horizontal | 0.2 | 1.15 | 1.5 | Middle- Horizontal | Model reconstruction and validation |
| B | 1 | Middle - Horizontal | 0.2 | 0.575 | 1.5 | Middle- Horizontal | Effect of inlet velocity |
| C | 1 | Middle - Horizontal | 0.2 | 2.3 | 1.5 | Middle- Horizontal | Effect of inlet velocity |
| D | 0 | - | - | - | 1.5 | Middle- Horizontal | No inlet pipe, only draft velocity |
| E | 1 | Middle - Horizontal | 0.2 | 1.15 | 0 | Middle- Horizontal | Effect of inlet velocity, no draft velocity |
| F | 1 | Side- Horizontal | 0.2 | 1.15 | 1.5 | Middle- Horizontal | Effect of inlet pipe position |
| G | 1 | Side - Horizontal | 0.2 | 1.15 | 1.5 | Middle- Horizontal | Effect of inlet pipe position |
| H | 1 | Side - Horizontal | 0.2 | 1.15 | 0 | Middle- Horizontal | Effect of inlet pipe position and no draft tube |

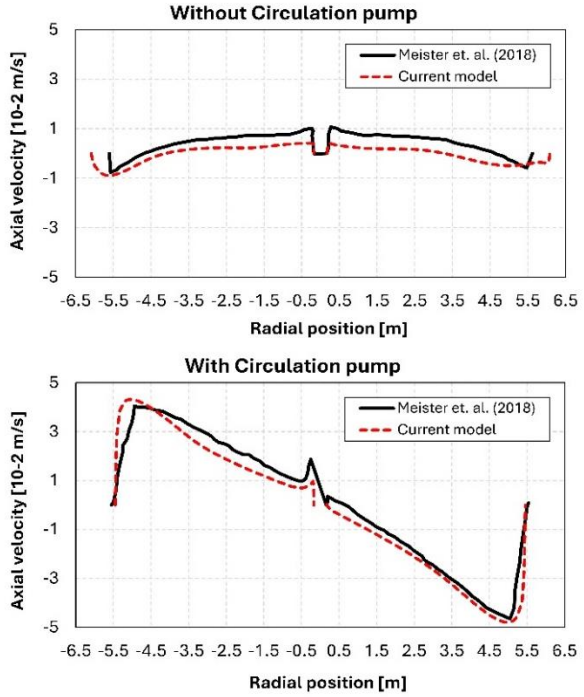


**Fig. 3.** Velocity profiles 6 m above the bottom– current model vs Meister *et. al.,* (2018).

### 3.2. Effect of inlet velocity

A series of simulations is conducted to investigate the impact of inlet velocity (without any geometrical modifications). The cases are tagged B and C for 0.575 and 2.3 m/s of inlet velocity respectively. Fig. 5 depicts the contour velocity magnitude, upward velocity, UI and TI for cases A, B and C.

As can be seen higher inlet velocity can noticeably increase the average velocity magnitude and also creates a more asymmetric upward velocity profile inside the mixing tank. This in itself can increases the mixing intensity however it reduces the uniformity of the flow inside the tank (increasing UI). As depicted in Fig. 6, higher inlet velocity can also create a more uniform and intense clockwise circulation which in turn can increase the intensity of the mixing process. Quantitative value of average velocity ($U_{ave}$), UI and TI are reported in Fig. 7 for a better analysis. Therefore, increasing the inlet velocity (Case C) seems to have a positive effect on the TI with a negligible increase in UI.

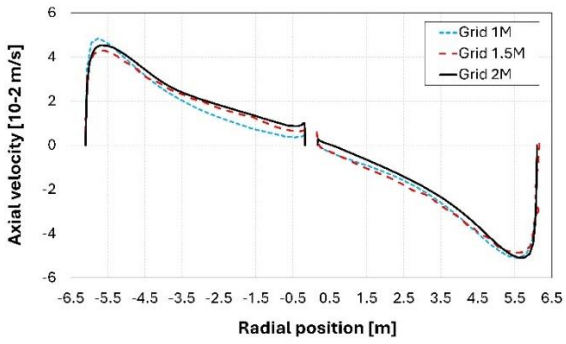


**Fig. 4.** Velocity profile for different computational grid (6 m above the bottom of digester).

**Table 3**. Obtained parameters for different computational grid.

| Cell count | $U_{ave}$ | UI | TI, % |
|---|---|---|---|
| 1 Million | 0.0295 | 0.64 | 0.580 |
| 1.5 Million | 0.0280 | 0.47 | 0.710 |
| 2 Million | 0.0285 | 0.48 | 0.706 |

### 3.3. Effect of draft tube recirculation

In another set of simulations, the effect of the draft tube on the average flow behavior is investigated. In one case (Case D), the inlet velocity is assigned to zero while the draft tube works as normal and in another case (Case E), the inlet velocity is active while draft tube momentum source is set to zero. As can be seen in Fig. 8, in case D where only draft tube is active a more symmetrical flow pattern is generated with a more symmetrical UI and TI distribution. Case D also provides a lower average UI and a higher averaged TI which points to a better performance of the digester (see Fig. 7). Once the inlet pipe is activated, the mixing and velocity vector pattern are switched to a clockwise pattern. When the draft tube is off, the same pattern is formed but in a more intensified pattern. Cases A and E led to the conclusion that the draft tube can adversely affect the circulation intensity produced by inlet flow by a perpendicular interaction with the inlet jet and reducing its velocity.

### 3.4. Effect of inlet tube position

Another set of simulations is carried out to examine the effects of the inlet tube positioning. Two different modifications are studied as sown in Fig. 9.

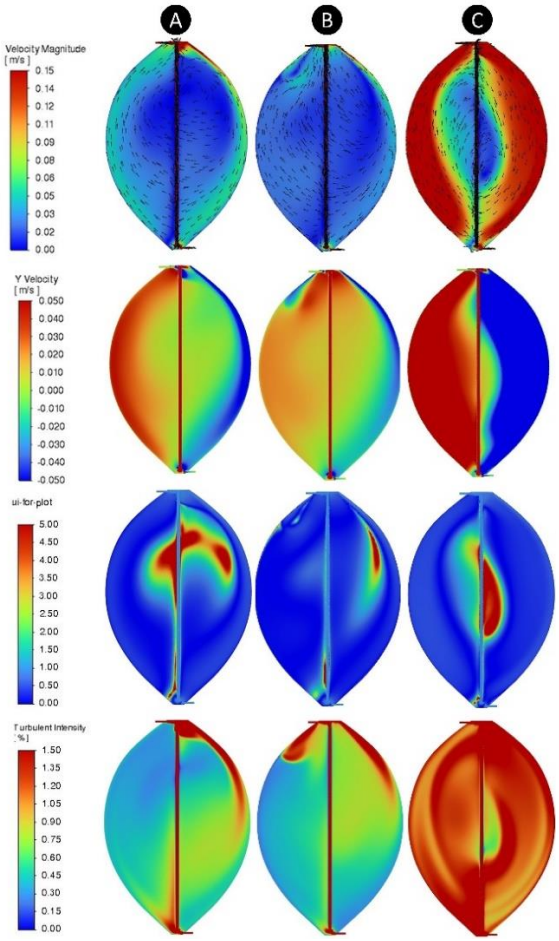


**Fig. 5**. Contour of velocities, UI and TI for different inlet velocities (Cases A, B and C).

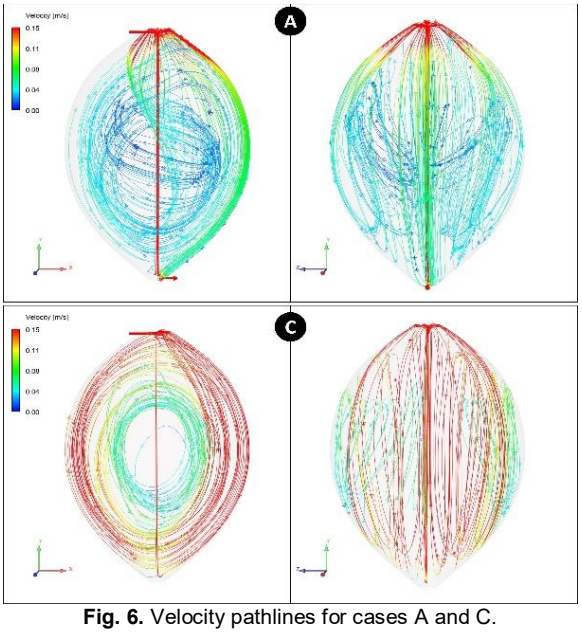


**Fig. 6.** Velocity pathlines for cases A and C.

All other boundary conditions are the same as the base case. The immediate effect of this configuration is its capability of inducing swirl motion within the tank. Fig. 10 shows the planar velocity vector at different cross-sections of the tank for Cases F and G. In both cases, the swirl motion is evident. As can be seen in Case F, the tube is positioned in the peripheral region of the digester and is inserted 46 cm into the tank. In Case G, the inlet tube is at the same position as in Case F; however, the tube is not inserted into the tank, and the tip of the tube is practically omitted once it touches the body of the tank.

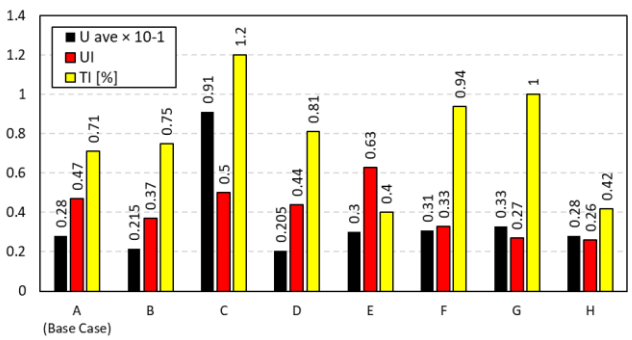


**Fig. 7.** Quantitative results of $U_{ave}$, UI and TI for different case studies.

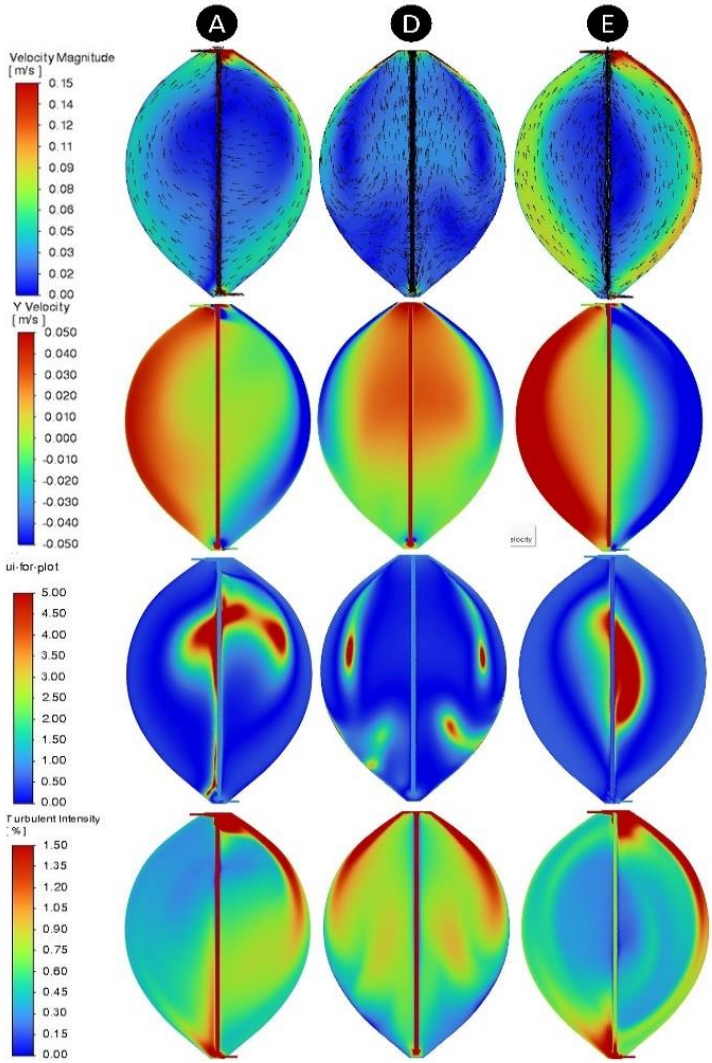


**Fig. 8.** Contour of velocities, UI and TI for different draft tube functions.

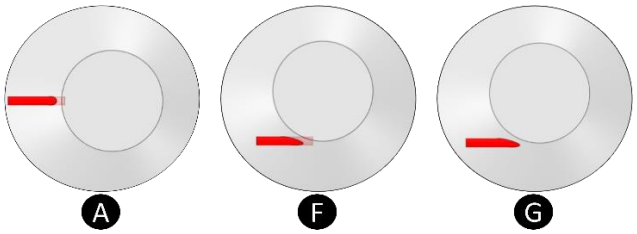


**Fig. 9.** Inlet tube position for cases F and G.

All other boundary conditions are same as the base case. The immediate effect of this configuration is its capability of inducing swirl motion within the tank. Fig. 10 shows the planar velocity vector at different cross-sections of the tank for Cases F and G. In both cases, the swirl motion is evident. Fig. 11 shows a better visualization using the velocity streamlines, and as can be seen, compared to Case A, the swirl motion is perfectly induced from the bottom to the top part of the digester tank. The reason for this swirl motion is the fact that the liquid is injected from the peripheral side of the tank, and due to the semi-spherical shape of the tank, the liquid swirls around the wall of the tank at high speed, inducing the same velocity profile in the radial direction. This is the same effect as in cyclone separators, which use a preferential air stream to create swirl motion inside the cyclone.

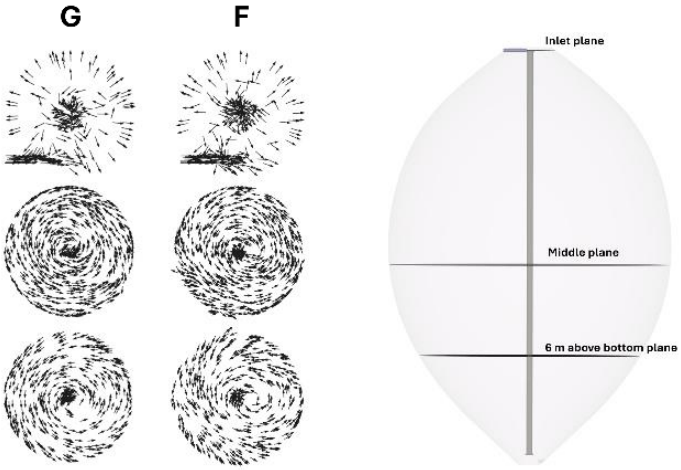


**Fig. 10.** Planar velocity vector for cases F and G.

The induced swirl motion in both cases F and G leads to higher TI and lower UI (more uniform flow) by achieving more or less the same average velocity within the digester once compared to Case A as reported in Fig. 7. Compared to Case F, slightly higher TI and lower UI is obtained for Case G. the reason for this advantage is the fact that in case G, the swirl motion of the liquid starts immediately after the liquid enters the tank while in Case F, due to the inserted tip of the tube, the first travels in a straight line first before getting into the swirl motion. Figure shows the aforementioned phenomena.

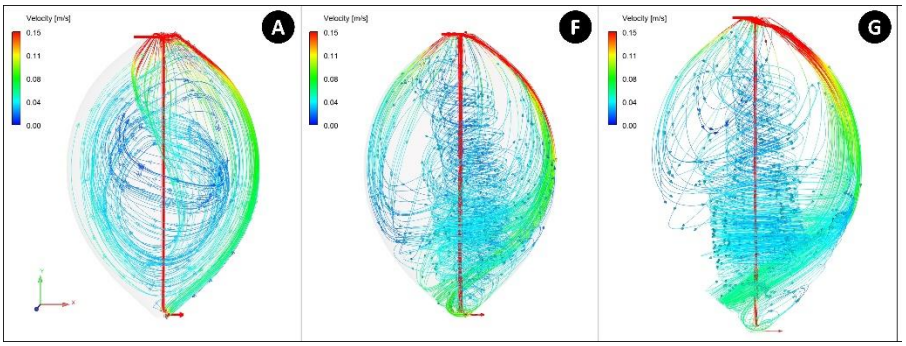


**Fig. 11.** Velocity streamline for cases A, F and G.

### 3.5. Effect of Newtonian and non-Newtonian fluid assumption

A set of simulations is performed to emphasize the importance of the non-Newtonian viscosity consideration for the current slurry flow. Properly accounting for the properties of non-Newtonian fluids in CFD is crucial because these fluids exhibit variable viscosity that depends on shear rate, which can significantly influence the flow behavior. Ignoring these properties by assuming a constant viscosity can lead to incorrect flow patterns and recirculation zones, inaccurate scaling of turbulence and instabilities, inconsistency in pressure drop and energy consumption, inaccurate heat and mass transfer factors, and potentially compromise the validity of the analysis and engineering decisions based on it. To better quantify the discussion, different cases for TS = 7.5% and 12.5% are considered, with and without a non-Newtonian viscosity model. Due to higher viscosity compared to the TS = 2.5% case, a higher momentum source is considered to reach the same average velocity inside the draft tube. This means that once the viscosity is increased, impeller power and rotation speed have to be increased, as also discussed by Meister *et al*. (2018). Case 1 is modelled with non-Newtonian consideration, and Case 2 is modelled using a constant viscosity value obtained from the average viscosity of Case 1 inside the tank.

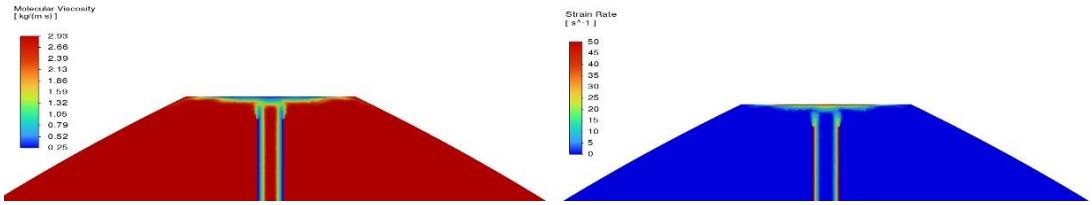


**Fig. 12.** Viscosity and strain rate contour for TS = 12.5% considering non-Newtonian fluid.

As can be seen in Fig. 12, using non-Newtonian relation, the flow viscosity is predicted to be lower inside the draft tube compared to the rest of the tank. This is due to the fact that in the current case studies, the slurry flow exhibit shear-thinning behavior (n<1 in equation) which means lower viscosity in areas with high shear strain like walls and low velocity regions. This effect will be neglected once a Newtonian fluid with a constant viscosity is considered and therefore, case 2 is indeed a failure to model viscosity characteristic which ultimately leads to incorrect predictions of flow rates and velocity profiles inside the draft tube. The difference between different calculated parameters are shown in Table 4. This discrepancy between values are more pronounced when TS content of the slurry flow is increased.

**Table 4.** Different calculated ammeter for different TS and viscosity models.

| Case D TS, % | Momentum source, N/m$^3$ | Average viscosity, Pa. s | | Average velocity, m/s | | TVR | | TI, % | |
|---|---|---|---|---|---|---|---|---|---|
| | | Draft tube | Tank | Draft tube | Tank | Draft tube | Tank | draft tube | Tank |
| Case 1 - 7.5% non-newtonian | 152 | 0.151 | 0.17 | 1.35 | 0.006 | 7.45 | 8.5 | 13.1 | 0.48 |
| Case 2 - 7.5% newtonian | 152 | 0.17 | 0.17 | 1.13 | 0.0036 | 7.2 | 5.8 | 11.8 | 0.37 |
| Case 1 - 12.1% non-newtonian | 350 | 1.45 | 2.93 | 1.42 | 0.0019 | 0.0015 | 0.003 | 1.5 | 0.08 |
| Case 2 - 12.1% newtonian | 350 | 2.93 | 2.93 | 0.45 | 0.0005 | 1.00E-08 | 1.00E-06 | 0.0125 | 0.0014 |

Assuming a constant viscosity in the current case, where a shear-thinning fluid is modelled, the viscosity inside the draft tube is artificially high even at the highest shear rates. This has led to a lower average velocity within the draft tube, which ultimately overpredicts the pumping energy required for flow circulation and leads to oversized equipment estimations. Another important inaccuracy that can emerge by considering a constant viscosity is the underestimation of turbulence inside the tank. To quantify the turbulent behavior of the flow, the turbulent viscosity ratio (TVR) is utilized here, which is the ratio of turbulent viscosity to the molecular (or dynamic) viscosity (TVR = $\eta t/\eta$). TVR can provide insight into the nature of the flow, whether it is laminar or turbulent. In laminar flow, turbulence is negligible, and the molecular viscosity is the sole contributor to momentum transport. For such a flow, the turbulent viscosity ratio should approach zero or remain low because the turbulent viscosity is either nonexistent or negligible compared to molecular viscosity. A turbulent viscosity ratio close to 1 or less would generally indicate negligible turbulence effects. A high turbulent viscosity ratio (ranging from 10 to 1000 or more) suggests strong turbulence, where the turbulent viscosity dominates the molecular viscosity.

As can be seen in Fig. 13 for case 2, the TVR is spatially and on average (Table 4) much lower than the case 1 where correct definition of non-Newtonian fluid is considered. In general, turbulence in slurry flow depends on the interaction between viscous forces and inertial forces. A fixed viscosity oversimplifies the interaction, especially for shear-thinning flow. Shear-thinning slurries can suppress turbulence in high-shear regions, such as the draft tube region, due to reduced viscosity, leading to errors in turbulent kinetic energy and dissipation rate predictions, which ultimately mispredict mixing efficiency.

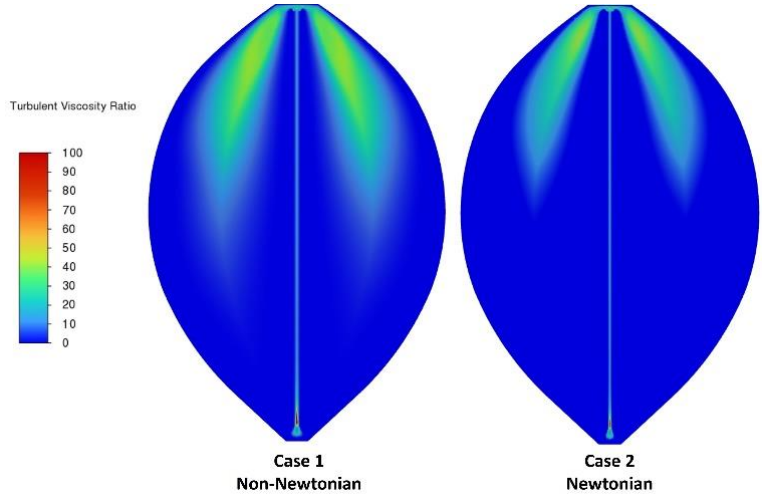


**Fig. 13.** Turbulent viscosity ratio contour for case 1 and 2 for TS = 7.5%.

## 4. Conclusions

This study employed CFD modeling to investigate and improve the mixing characteristics of an egg-shaped anaerobic digester in a wastewater treatment plant. The results demonstrate that optimizing operational and geometric parameters, particularly inlet velocity, draft tube design, and pipe positioning, plays a critical role in enhancing flow uniformity and turbulence within the digester. Simulations confirmed that adjusting the inlet velocity strongly influences mixing dynamics: higher velocities increase turbulence intensity and improve circulation, but they can also reduce flow uniformity and lead to less efficient mixing, highlighting the need for careful balance between turbulence and uniformity. The draft tube was shown to be an important feature for generating symmetrical flow patterns and improving mixing efficiency, although in some cases its interaction with the inlet flow disrupted circulation and caused localized velocity reduction. Overall, the draft tube contributed positively to maintaining stable mixing dynamics, particularly under moderate inlet velocity conditions. Inlet pipe positioning was found to exert a significant influence on flow distribution. Peripheral configurations, in combination with the egg-shaped geometry of the digester, induced swirl motion that enhanced turbulence and reduced dead zones, thereby improving overall mixing efficiency with minimal design modifications. The quantitative evaluation of mixing performance using the uniformity index and Turbulence Intensity further demonstrated that proper tuning of inlet velocity, draft tube function, and pipe placement can reduce stagnant regions, enhance circulation, and improve mixing uniformity. Such improvements directly contribute to more effective anaerobic digestion and biogas production. Looking forward, future work should aim to couple CFD hydrodynamics with additional physical and biochemical processes, including gas–liquid interactions, heat transfer, and digestion kinetics, to achieve a more comprehensive representation of digester performance. Incorporating microbial transport, substrate distribution, and population balance models could provide valuable insights into how mixing affects digestion efficiency at the micro-scale, while transient simulations would capture the effects of fluctuating influent loads, startup phases, and intermittent mixing cycles. Such developments would enable a more realistic assessment of plant operations, improve predictions of biogas yield under dynamic conditions, and support the design of more efficient, robust, and sustainable anaerobic digestion systems.

## Author Contributions

Seyed Hosein Arabfarashahi: Conceptualization, Formal Analysis, Methodology, Software, Original Draft Preparation.
Shahram Talebi: Conceptualization, Methodology, Review and Editing, Supervision.

## Conflict of Interest

The authors declare no conflict of interest.

## Acknowledgement

The author acknowledges the Energy Conversion Group, Department of Mechanical Engineering, Yazd University, Yazd, Iran.

## Data Availability Statement

The data supporting the findings of this study were generated through computational fluid dynamics (CFD) simulations. The simulation input files and post-processing results are available from the corresponding author upon reasonable request.

## References

ANSYS, Inc. (2024) ANSYS Fluent Theory Guide, Release 2024, ANSYS, Inc., Canonsburg.

Caillet, H., Bastide, A. and Adelard, L. (2023) 'Advances in Computational Fluid Dynamics modeling of anaerobic digestion process for renewable energy production: A review', *Cleaner Waste Systems*, 6, p. 100124. doi: https://doi.org/10.1016/j.clwas.2023.100124

Craig, K.J., Nieuwoudt, M.N. and Niemand, L.J. (2013) 'CFD simulation of anaerobic digester with variable sewage sludge rheology', *Water Research*, 47(13), pp. 4485–4497. doi: https://doi.org/10.1016/j.watres.2013.05.011

Dabiri, S. *et al.* (2021) 'CFD modeling of a stirred anaerobic digestion tank for evaluating energy consumption through mixing', *Water (Basel)*, 13(12). doi: https://doi.org/10.3390/w13121629

Hernandez-Aguilar, E. *et al.* (2016) 'Development of energy efficient mixing strategies in egg-shaped anaerobic reactors through 3D CFD simulation', *Journal of Environmental Science and Health, Part A*, 51(7), pp. 536–543. doi: https://doi.org/10.1080/10934529.2016.1141619

Karim, K., Varma, R., Vesvikar, M. and Al-Dahhan, M.H. (2004) 'Flow pattern visualization of a simulated digester', *Water Research*, 38(17), pp. 3659–3670. doi: https://doi.org/10.1016/j.watres.2004.06.009

Leonzio, G. (2018) 'Study of mixing systems and geometric configurations for anaerobic digesters using CFD analysis', *Renewable Energy*, 123, pp. 578–589. doi: https://doi.org/10.1016/j.renene.2018.02.071

López-Jiménez, P.A. *et al.* (2015) 'Application of CFD methods to an anaerobic digester: The case of Ontinyent WWTP, Valencia, Spain', *Journal of Water Process Engineering*, 7, pp. 131–140. doi: https://doi.org/10.1016/j.jwpe.2015.05.006

Meister, M. *et al.* (2018) 'Mixing non-Newtonian flows in anaerobic digesters by impellers and pumped recirculation', *Advances in Engineering Software*, 115, pp. 194–203. doi: https://doi.org/10.1016/j.advengsoft.2017.09.015

Meroney, R.N. and Colorado, P.E. (2009) 'CFD simulation of mechanical draft tube mixing in anaerobic digester tanks', *Water Research*, 43(4), pp. 1040–1050. doi: https://doi.org/10.1016/j.watres.2008.11.035

Sajjadi, B., Raman, A.A.A. and Parthasarathy, R. (2016) 'Fluid dynamic analysis of non-Newtonian flow behavior of municipal sludge simulant in anaerobic digesters using submerged, recirculating jets', *Chemical Engineering Journal*, 298, pp. 259–270. doi: https://doi.org/10.1016/j.cej.2016.03.069

Stamou, A.I. (2008) 'Improving the hydraulic efficiency of water process tanks using CFD models', *Chemical Engineering and Processing: Process Intensification*, 47(8), pp. 1179–1189. doi: https://doi.org/10.1016/j.cep.2007.02.033

Terashima *et al*. (2009) 'CFD simulation of mixing in anaerobic digesters', *Bioresource Technology*, 100(7), pp. 2228–2233. doi: https://doi.org/10.1016/j.biortech.2008.07.069

Wols, B.A. *et al*. (2010) 'Evaluation of different disinfection calculation methods using CFD', *Environmental Modelling and Software*, 25(4), pp. 573–582. doi: https://doi.org/10.1016/j.envsoft.2009.09.007

Vesvikar, M.S. and Al-Dahhan, M. (2005) 'Flow pattern visualization in a mimic anaerobic digester using CFD', Biotechnology and Bioengineering, 89(6), pp. 719–732. doi: https://doi.org/10.1002/bit.20388

Wu, B. (2014) 'CFD simulation of gas mixing in anaerobic digesters', *Computers and Electronics in Agriculture*, 109, pp. 278–286. doi: https://doi.org/10.1016/j.compag.2014.10.007

Singh, B. *et al.* (2021) 'Critical analysis of methods adopted for evaluation of mixing efficiency in an anaerobic digester', *Sustainability*, 13(12). doi: https://doi.org/10.3390/su13126668

Van Canneyt, K. and Verdonck, P. (2014) '10.02 - *mechanics of biofluids in living body', in comprehensive biomedical physics*, A. Brahme, Ed., Oxford: Elsevier, pp. 39–53. doi: https://doi.org/10.1016/B978-0-444-53632-7.01003-0

Wang, F., Zhang, C. and Huo, S. (2017) 'Influence of fluid dynamics on anaerobic digestion of food waste for biogas production', *Enviromental Technology*, 38(13), pp. 1681-1688. doi: https://doi.org/10.1080/09593330.2016.1220429

Wu, B. (2010) 'CFD simulation of mixing in egg-shaped anaerobic digesters', *Water Research*, 44(5), pp. 1507–1519. doi: https://doi.org/10.1016/j.watres.2009.10.040

Zhang, J. *et al.* (2018) 'Structural characteristics of a spiral symmetry stream anaerobic bioreactor based on CFD', *Biochemical Engineering Journal*, 137, pp. 50–61. doi: https://doi.org/10.1016/j.bej.2018.05.016